

# Experimental Studies on the Fixed Force of Anchor Pile in the Sea Bed

## III. Structures of Sandy Ground and Limit Resistance Force of Anchor Pile in the Field Experiments

Yukihiro MUNEKAGE and Seiji TOCHIKI

*Laboratory of Fisheries Engineering, Faculty of Agriculture*

**Abstract :** In this paper, the use of piling as a possible means of anchoring such equipment as floating breakwaters, oyster rafts, fish preserves, etc. was investigated.

The structures of sandy ground of the sea bottom were examined by means of a handy dynamic cone penetrometer – a device in which a known movable weight is allowed to fall from a predetermined height over the upper rod of the penetrometer, slamming into a shoulder to give a measured amount of force on the cone of the penetrometer. The characteristics of the sandy ground were inferred from the number of blows necessary to penetrate a given depth.

Two types of ground were discovered. The hardness of Type -I increases constantly with depth. Type -II has a constant hardness below a certain depth.

The effect of both the limit resistance force and the bending moment were measured and reported. Varying the point of loading the pile was also investigated. It was found that placing the load point about twenty five percent of the embedded length below ground level both reduced the bending moment and increased the limit resistance to optimum.

### Introduction

It is very important to solve the problem of anchoring equipment used in cultivating fisheries in the sea ; such as floating breakwaters, rafts for oyster farming, fish preserves, and so on.

Up to this time, steel anchors, concrete anchors, and something like sand bags have been always used. However it is desired that an anchoring system which has long life, good stability and is easy to construct be developed.

In this report, the use of piles driven into the sea bed was investigated. First of all, the dynamic characteristics of the sandy ground in the sea bed were determined. Then, while the pile was being horizontally pulled at ground level in the sea bed, by a gradually increasing tension force, the limit resistance force of the anchor pile just at the time of extraction was measured.

By model experiments, the general characteristics of the relationship between the limit resistance force and the following three variables were determined : (1) the density or hardness of sandy ground, (2) the diameter of pile, (3) the embedded length of the pile below the sea bed. We also tested its practical use by means of field experiments.

The experiments also indicated that the anchoring force was increased (30–35 %) by pulling on the pile at a point about one fourth of the embedded depth.

### Experimental method

#### 1. Piles used in the experiments

Iron piles varying in length from 30 to 50 cm, and in thickness from 0.6 to 2.5 cm were

used. Circular, square and deformed shapes were tested, as shown in Table 1, in the model experiments. In the field experiments, round, hollow manufactured iron piles varying in length from 80 to 162 cm, and in diameter from 3.4 to 10.2 cm, were used, as shown in Table 2. These piles were used for measuring the limit resistance force.

Vinyl chloride pipes, as shown in Table 3, were also used in order to examine the bending moment distributions of the piles which received horizontal tension. Strain gauges were attached to the model pile every 5 cm, and the strain on the pile recorded in both sandy and clay ground experiments. The bending moment was then calculated.

Table 1. Details of model piles for model experiments

Pile No	Diameter or Side length (cm)	Pile length (cm)	Shape
L-1	1.70	50.0	Circular
2	1.40	45.0	
3	2.50	45.0	
4	1.61	47.0	
5	1.24	47.0	
6	2.00	45.0	
7	0.86	47.0	
8	0.93	47.0	Square
9	1.35	46.5	
10	2.05	47.0	Deformed
11	0.60	46.0	Circular
S-1	1.40	30.0	
2	1.70	30.0	
3	1.60	30.0	
4	1.20	30.0	
5	0.80	30.0	
6	1.00	30.0	
7	0.60	30.0	
8	0.60	30.0	Square
9	0.80	30.0	
10	1.00	30.0	
11	1.20	30.0	

Table 2. Details of piles for field experiments

Pile No	Diameter (cm)	Pile length (cm)	Shape
L-1	7.70	161.5	Circular
2	8.80	161.0	
3	10.20	161.0	
M-1	3.40	126.0	Circular
2	4.30	126.0	
3	6.00	124.0	
4	7.70	121.0	
5	8.80	121.0	
6	10.20	121.0	
S-1	3.40	80.0	Circular
2	4.20	80.0	
3	6.00	80.0	
4	7.70	80.0	
5	8.80	80.0	
6	10.20	80.0	

Table 3. Characteristics of model piles for measuring the bending moment distribution

Pile-No	Diameter (cm)		Length (cm)	E kg/cm <sup>2</sup>	I cm <sup>4</sup>	EI kg/cm <sup>2</sup>	Z cm <sup>3</sup>	EZ kg/cm	Slenderness ratio
	Outside	Inside							
Pile-1	2.60	2.02	32.0	$2.366 \times 10^4$	1.426	$3.374 \times 10^4$	1.096	$2.593 \times 10^4$	220
Pile-2	1.80	1.32	32.0	$2.738 \times 10^4$	0.366	$1.002 \times 10^4$	0.407	$1.114 \times 10^4$	267
Pile-3	2.60	2.02	46.0	$2.366 \times 10^4$	1.426	$3.374 \times 10^4$	1.096	$2.593 \times 10^4$	317

2. Handy dynamic cone penetrometer (for experimental purposes)

The authors made the handy dynamic cone penetrometer used in the experiments, in order to investigate the density or hardness of the sandy ground easily. Something like this penetrometer was made by Okubo et al.<sup>1)</sup> for the purpose of carrying out ground investigation on steep slopes under difficult conditions. In this experiment, we made a smaller type as shown in Fig. 1.

We dropped a 2 kg weight from 10 cm high, and expressed the density or hardness of the ground as  $N$ , (i.e. the number of blows which were necessary to cause the cone shaped end of the rod (Fig. 1) to penetrate a depth of 10cm.) In the field experiments, we dropped a 4 kg weight from 20 cm high.

In changing the percussion energy as above, the  $N$  value also changed even under the same ground conditions. (These experiments were carried out on the beach at Tei which has very constant ground characteristics.) Fig. 2 shows the effect of changing the applied energy on the value of  $N$  as the depth increased. At a given depth in Fig. 2,

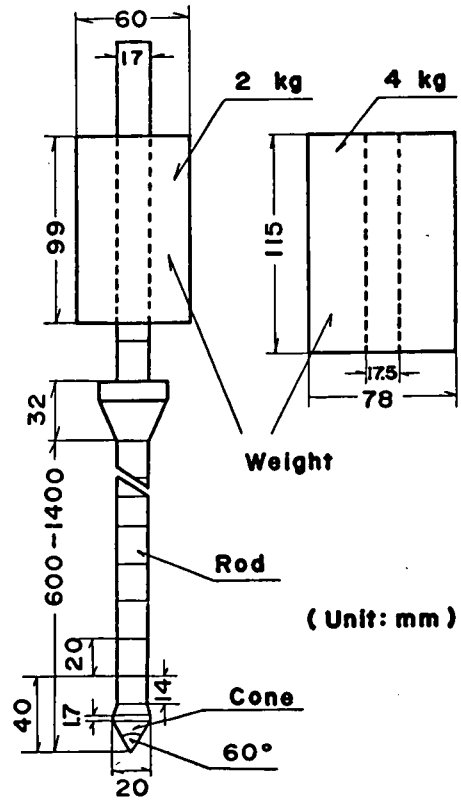


Fig. 1. Handy dynamic cone penetrometer for experiment.

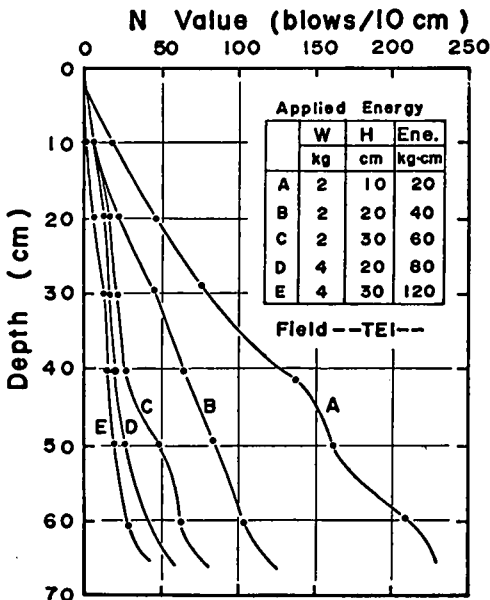


Fig. 2. Effect of changing applied energy on the value of  $N$ .

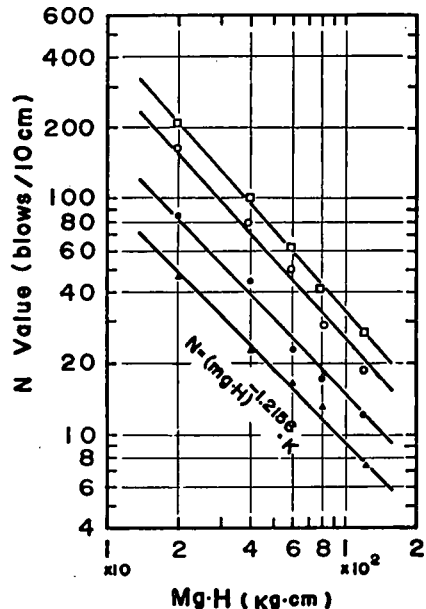


Fig. 3. Effect of increasing applied energy on number of blows  $N$ .

we can express the effect of increasing the applied energy on the number of blows  $N$  as shown in Fig. 3. Fig. 3 shows that the increase of percussion energy decreases the  $N$  value exponentially.

In Fig. 3, the value of  $N$  is given by

$$N = (Mg \cdot H)^a \cdot K \quad \dots\dots\dots (1)$$

where  $N$  = number of blows necessary to penetrate 10 cm at any depth ;  
 $Mg$  = weight in kg ; and  
 $H$  = height in cm.

in which  $a$  is a constant, and  $K$  is connected with the difference of ground condition. The value of  $K$  explains the penetration resistance, the density or hardness of the sandy ground under the same ground conditions, in the case where  $Mg \cdot H = 20$  kg. cm percussion energy is added,

$$N_{20} = (Mg \cdot H_{20})^a \cdot K$$

and where  $Mg \cdot H = 80$  kg. cm,

$$N_{80} = (Mg \cdot H_{80})^a \cdot K$$

$K$  can be eliminated from both the above equations, and rearranged, resulting in the following equation :

$$N_{20} = (Mg \cdot H_{20} / Mg \cdot H_{80})^a \times N_{80} \quad \dots\dots\dots (2)$$

in which the constant  $a$  has already been determined as  $a = -1.2156$  in Fig. 3, and finally, eq. (2) reduces to

$$N_{20} = (Mg \cdot H_{20} / Mg \cdot H_{80})^a \times N_{80} = (20/80)^{-1.2156} \times N_{80} = 5.393 \times N_{80} \quad \dots\dots\dots (3)$$

Consequently, even in cases in which the percussion energy is changed, the "standard" value of  $N$  can be calculated.

3. Sand used in the model experiments

The three kinds of comparative homogeneous sand, as shown in Fig. 4, were collected from the following three points in Kochi prefecture ; (A) The beach at Tei, (B) Near the

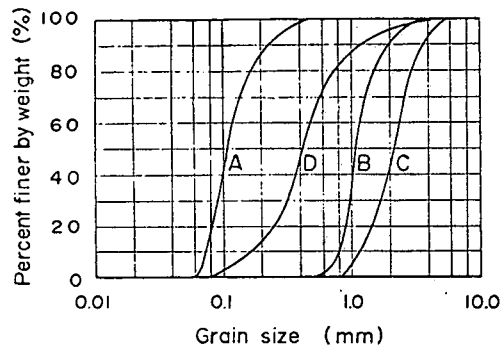


Fig. 4. Grain size distribution curve.  
 A:TEI, B: IRINO, C: NIYODO, D: URANOUCHI

beach at Irino, (C) Near the mouth of the Niyodo River.

These sands were used for the model experiments in a completely saturated condition. First of all, the ground characteristics were tested by means of the handy dynamic cone penetrometer. Then, while the embedded pile was being horizontally pulled, by a gradually increasing tension force, as shown in Fig. 5, the limit resistance force, angle of tension, and pile displacement angle just at the time of extraction were measured at the same time.

Field experiments were also carried out on the shallow sandy ground in the bay of Urano-uchi. The same tests as in the model experiments were repeated to investigate the limit resistance force automatically by use of the tension meter (which was a differential transformer type made by the Sakata Electric Co. having a maximum tension capacity of two tons).

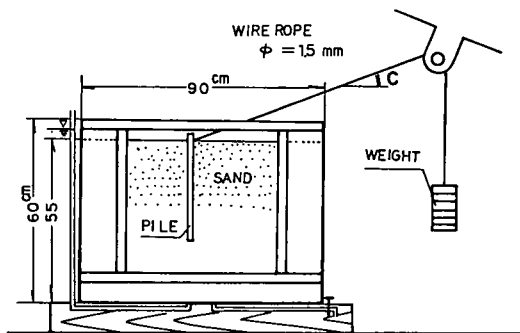


Fig. 5. Experimental equipment.

**Results and discussion**

1. Density or hardness of the sandy ground and its structures

In dropping the weight from the constant height, the quantity of cone penetration from

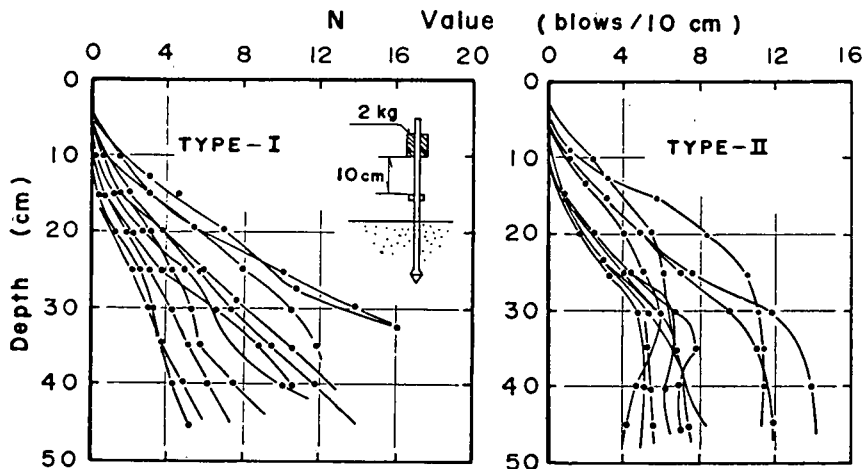


Fig. 6. N value in model experiment.

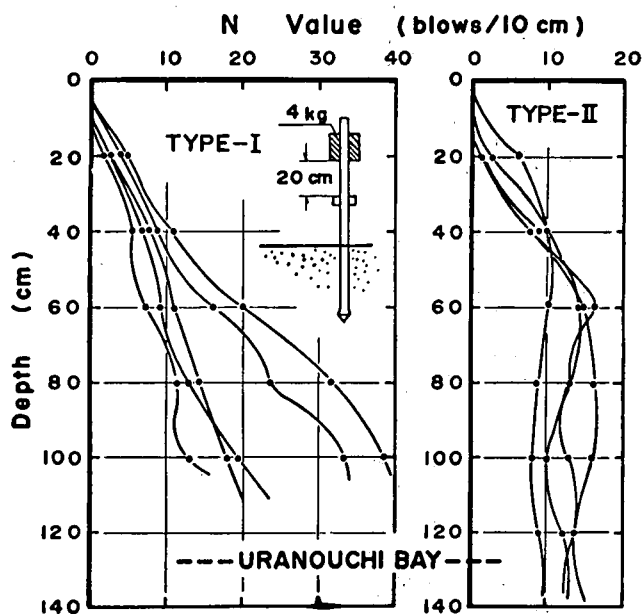


Fig. 7.  $N$  value in field experiment.

the ground surface was recorded after every drop. The graphic differential was plotted on the basis of 10 cm units by means of a graph which showed the relationship between the penetration depth and the total number of blows. Thus, the  $N$  values were determined.

Fig. 6 shows the results in the model experiments, and Fig. 7 in the field experiments. In both cases, sandy ground structures are distinguished into two types with regard to the hardness and the depth. Type - I shows that the hardness of the sandy ground increases constantly, and Type - II has a constant hardness below a certain depth. (This depth varies with location.) There were many cases of Type - II, especially in the field experiments.

## 2. Limit resistance force of anchor pile in sandy ground

In designing anchor piles, the relationship between the anchoring force of the pile  $F$  and the following three items make it possible to design a practical anchor pile :

- (1) Density or hardness of the sandy ground  $N$ ;
- (2) Cross section of the pile  $D$ ; and
- (3) Embedded length of the pile  $L$ .

In this report, the anchoring force of the pile is dealt with as the limit resistance force. The pile displacement angle  $d$  was measured at the same time that the limit resistance force was recorded, while changing the angle of tension  $c$  from  $5^\circ$  to  $43^\circ$ , in these experiments. The fact is that the tension force of  $F \cdot \cos(c+d)$  acts on the pile. Fig. 8 shows the relationship between the angle of tension and the constant  $\cos(c+d)$ .

Both (2) and (3) are dimensions of the pile. Generally, the shape of pile can be expressed as a nondimensional value  $D/L$ .

In these experiments, the following physical quantities were selected with reference to the anchoring force of the pile. Then, the following equation was obtained by use of dimensional

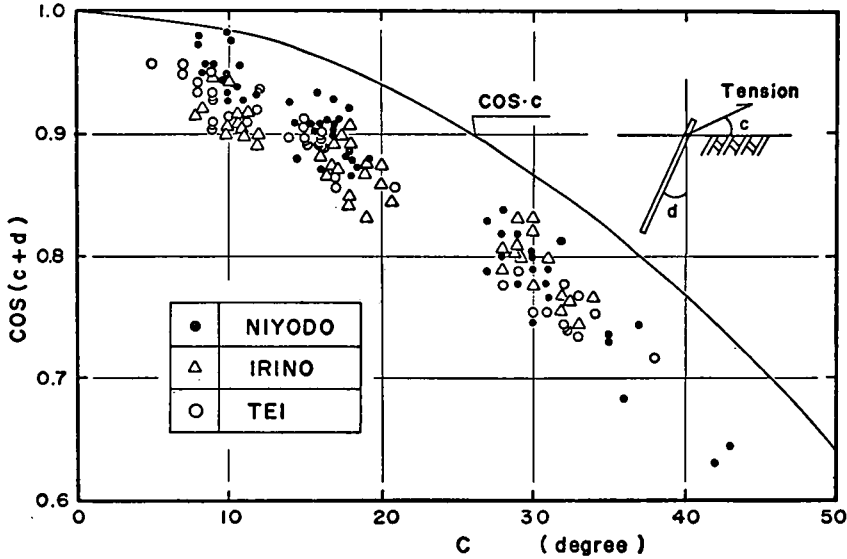


Fig. 8. Relation between  $C$  and  $COS(c+d)$ .  
 where,  $C$ =angle of tension,  $d$ =pile displacement angle at time of extraction.

analysis.

$$f(F \cdot COS(c+d) \cdot L/Mg \cdot H \cdot \Sigma N, L/h, D/L, D/d_{50})=0 \quad \dots\dots\dots (4)$$

in which nondimensional term  $F \cdot COS(c+d) \cdot L/Mg \cdot H \cdot \Sigma N$  is the ratio of the limit resistance force to the average density or hardness of the ground, and  $h$  is the depth at which the density or hardness becomes a constant condition, and  $d_{50}$  is the mean grain size of the sand.  $\Sigma N$  is the total number of blows which are necessary to cause the cone to penetrate up to certain depth  $L$ . The work  $W$  done by the percussion of  $\Sigma N$  is expressed as  $W=Mg \cdot H \cdot \Sigma N$ . The larger this value is, the harder the ground is, and the bigger the limit resistance force becomes.

In cases where  $\Sigma N$  is equal, as shown in Fig. 9, by the balance of moment, it seems that the Type - II ground is better in respect of the resistance force. Actually, in this case, the relationship between the  $N$  value and the depth is slightly more complex. However, in a ideal situation, the condition in ground of Type - II may be expressed as (see Fig. 9)

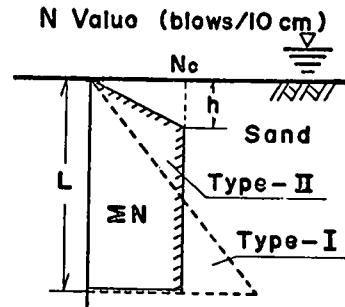


Fig. 9. Diagram illustrating the relationship between hardness of sand and limit resistance force of anchor pile.

\*\* In cases where  $\Sigma N$  is equal, limit resistance force of anchor pile in Type - I soil is greater than that in Type - II.

$$\Sigma N = \frac{N_c \times h}{2} + N_c \times (L-h)$$

$$\frac{\Sigma N}{L} = \frac{N_c}{L} \left( L - \frac{h}{2} \right) = N_c \left( 1 - \frac{h}{2L} \right)$$

in which  $N_c$  shows the constant hardness of the sandy ground. While  $N_c$  is constant, the

average hardness  $\Sigma N/L$  is inverse proportion to  $h$ . It is regarded that Type-I is in the condition of  $h \geq L$ , then it can be calculated as  $h=L$ .

And eliminating  $L$  from the 2nd and 3rd terms in eq. (4),

$$\pi_3' = \pi_2 \times \pi_3 = \frac{D}{h}$$

Finally, eq. (4) is rearranged into the next equation.

$$f(F \cdot \text{COS}(c+d) \cdot L / \text{Mg} \cdot H \cdot \Sigma N, D/h, D/d_{50}) = 0 \dots\dots\dots (5)$$

Fig. 10 shows the results of model experiments which were carried out by the use of three

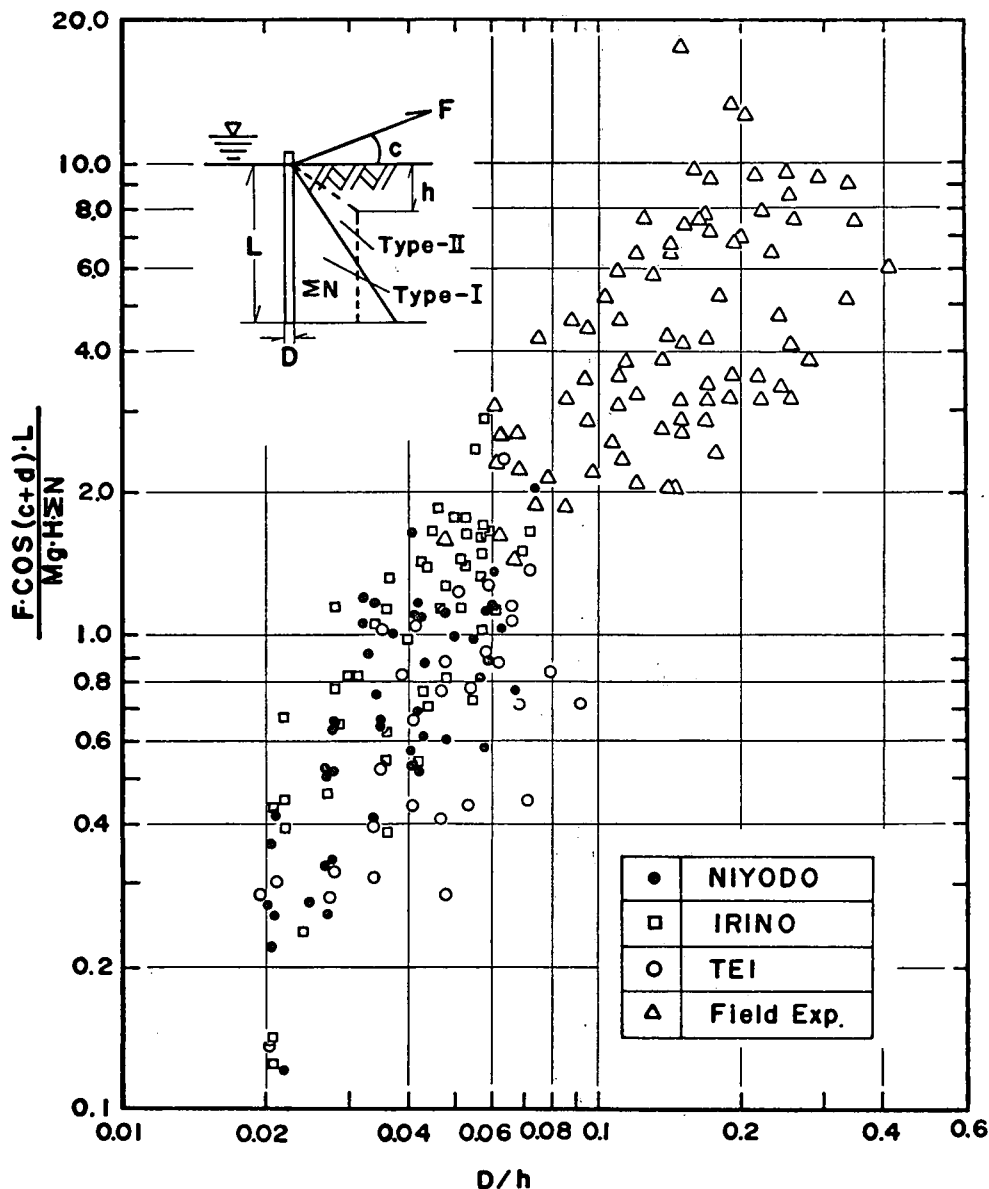


Fig. 10. Limit resistance force in saturated sand.



kinds of sand and of field experiments performed in the Bay of Uranouchi, according to eq. (5).

The difference in reference to the grain size of sand could not be identified clearly, but generally it shows good correlations. The results of the field experiments reproduce the trend which was shown in the model experiments.

3. Effect of moving the load point below ground level on the limit resistance force

When the pile receives tension below ground level, the limit resistance force is increased. Fig. 11 shows the effect of moving the load point on the limit resistance force. In this figure,  $F_a$  is the limit resistance force at the underground load point, and  $F_o$  is the limit resistance force at the ground level.  $D_o$  is the embedded depth, and  $D_a$  is the depth of the underground load point. In this case, the experiments were carried out in the same ground conditions as shown in Fig. 11, B. Fig. 11, A shows that the limit resistance force was increased about 30–35 % by pulling the pile at a point about one fourth of the embedded depth.

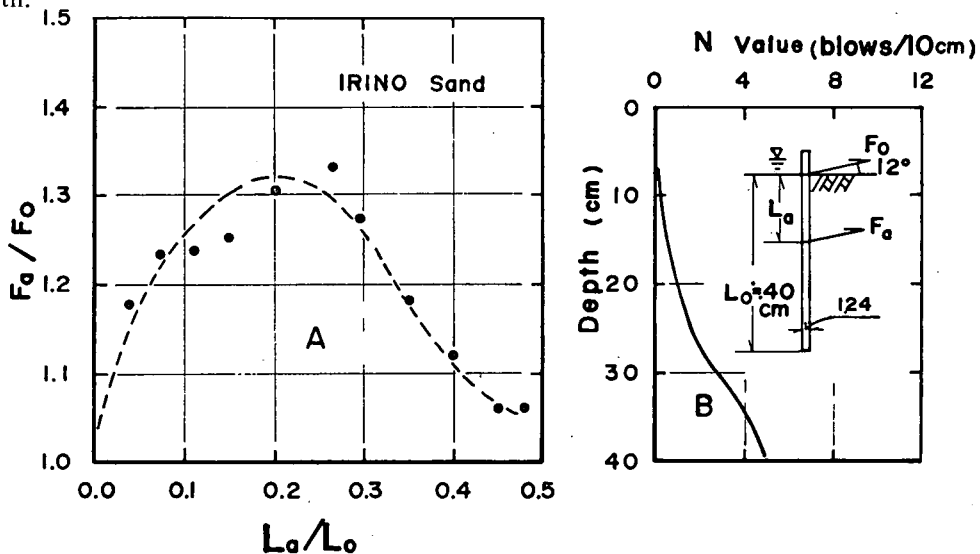


Fig. 11. Effect of moving load point below ground level on limit resistance force.  
 $F_a$  = Limit resistance force at underground load point.  
 $F_o$  = Limit resistance force at ground level.

4. Bending moment distribution of the pile

The strain was recorded by strain gauges attached to the pile, and then the bending moment was calculated in order to investigate the characteristics of pile deformation when the load point is moved various distances below ground level. When the load point is at ground level (as in Fig. 12, A), and a zero point of bending moment exists in the lower part of the pile, thereby creating bending moment of opposite directions within the pile, as though the lower end of the pile was fixed, the pile has been treated as a "long pile".

Fig. 12, B – Fig. 12, E show the different characteristics of bending moment distribution that occur in changing the load point below ground level.

Fig. 13 shows the effect of moving the load point on the distribution of bending moment. In Fig. 13,  $M_o$  is the maximum bending moment when the load point is at ground level,

and  $M_a$  is the maximum bending moment when the load point is below ground level.  $F_o$  is the limit resistance force at the ground level load point and  $F_a$  is the limit resistance force at the underground load point.  $D_o$  is the embedded depth of the pile and  $D_a$  is the depth of underground load point.

In this case of  $F_a/F_o=0.75\sim 1.25$  (shown by the solid black dots), the parabolic trend was obtained as shown by the dotted line in Fig. 13, with regard to the effect of moving the

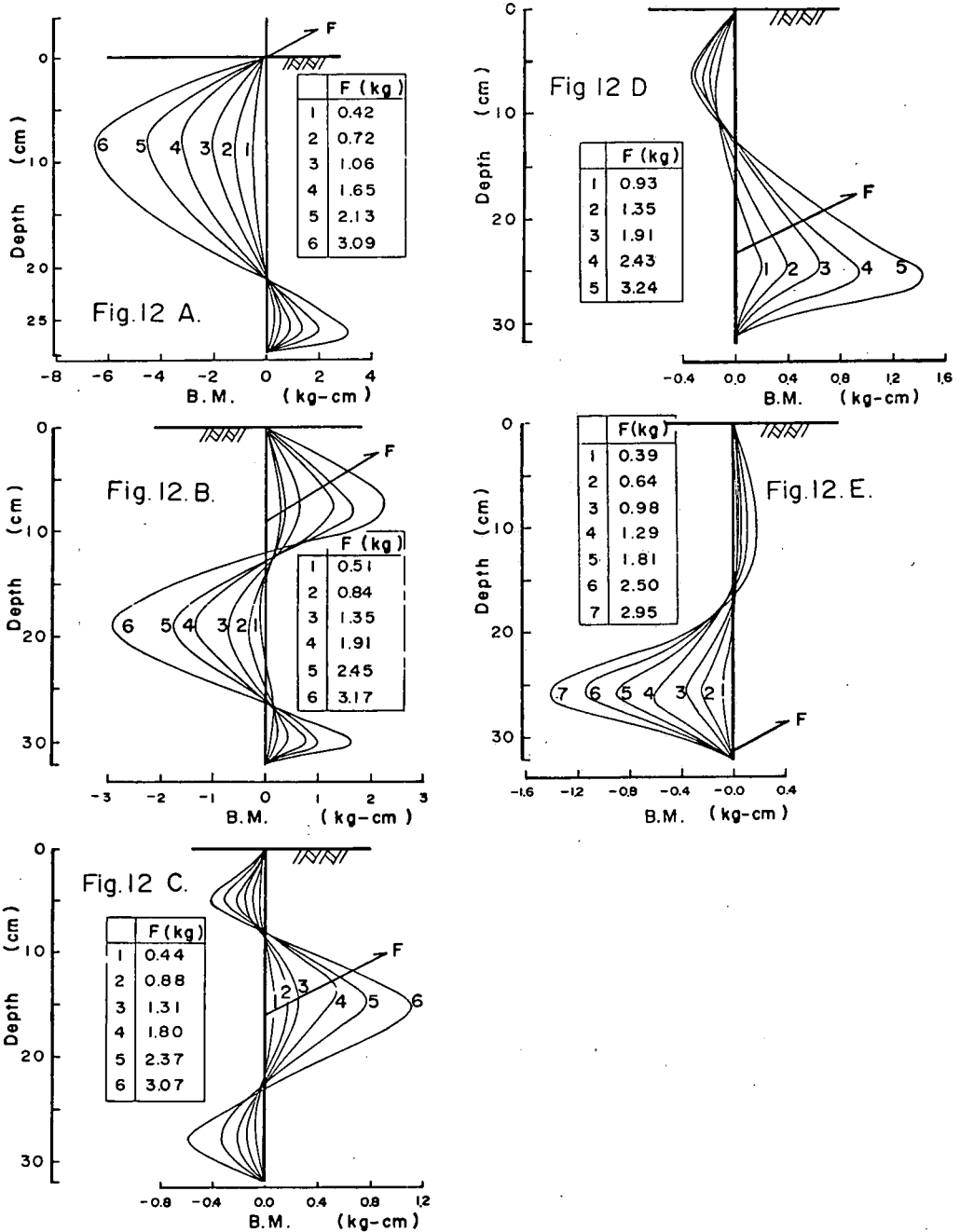


Fig. 12. Effect of moving load point on distribution of bending moment.

load point on the maximum bending moment.

In both bounds of  $D_a/D_o < 0.2$  and  $D_a/D_o > 0.8$ , the maximum bending moment has a negative value as at ground level, in  $0.2 < D_a/D_o < 0.8$ , it has positive value, and in  $D_a/D_o = 0.2, 0.8$ , it decreases to zero. Also, the absolute value of the maximum bending moment when pulling at the load point below ground level is much smaller than its counterpart when pulling at ground level.

These results show that moving the load point below ground level decreases the bending moment on the pile. Consequently, it is reasonable to design piles with a surplus of strength to guard against the destruction of the pile itself, also the optimum load point is 20–30 % of the embedded depth, at this point, maximum limit resistance force and minimum bending moment are achieved.

**Conclusions**

1. In order to investigate the hardness or the density of the sandy ground under the sea, the handy dynamic cone penetrometer as shown in Fig. 1 was made. The characteristics of sandy ground can be inferred by the number of blows which were necessary to cause the cone shaped end of the rod to penetrate a depth of 10 cm, when the weight is dropped from 10 cm high.

2. In these experiments, it was found that the sandy ground structure was distinguished into two types, with regard to the hardness and the depth. Type - I shows that the hardness of the sandy ground increases constantly. Type - II has a constant hardness below a certain depth.

3. The limit resistance force of the anchor pile in the sea bed was shown in Fig. 10, by use of nondimensional physical values in eq. (5). The results of the field experiments

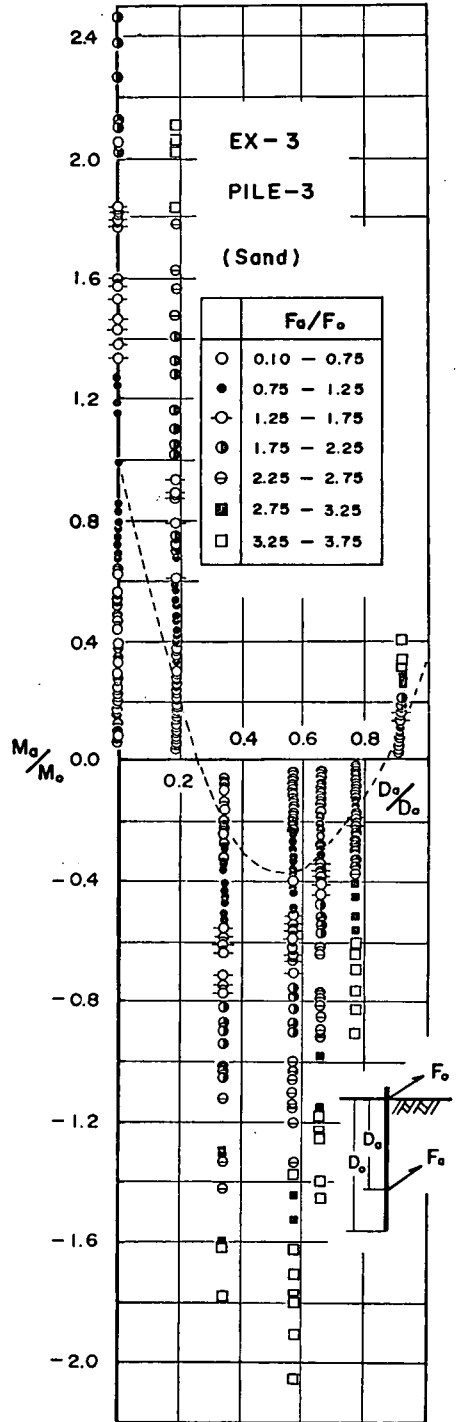


Fig. 13. Effect of moving load point below ground level on maximum bending moment.

reproduce the trend which was shown in the model experiments.

4. By pulling on the pile at a point about one fourth of the embedded depth below ground level, the limit resistance force was increased about 30–35 %.

5. When the load point is below ground level (as in 4 above), the absolute value of the bending moment on the pile becomes much smaller. It is then possible to design an economical anchor pile.

#### Acknowledgment

The writers are grateful to the Ministry of Agriculture and Forestry for the financial assistance provided as one of the studies for the shallow waters development project. Thanks are also given to Mr. D. G. Burney for assistance in the English translation.

#### References

- 1) S. Okubo, T. Kamisaka and M. Funazaki, The investigation method of surface layer on the slope using handy dynamic cone penetrometer. *Jisuberi*, 8 (4), 21–29 (1971).
- 2) S. Tochiki and Y. Munekage, Experimental studies on the fixed force of anchor pile in the sea bed (I), (II). *Reports of Kochi Univ.*, 21 (1), 1–14 (1972), 22 (9), 83–94 (1973).
- 3) Amin Awad, Consideration on the bearing capacity of vertical and batter piles subjected to forces acting in different directions, Hungarian Academy of Sciences, Proceeding of the 3rd Budapest conference on soil mechanics and foundation engineering, Oct. 15–18, 483–497 (1968).
- 4) S. Tochiki and Y. Munekage, Fixed force of anchor pile in the sea bed. *Fisheries Engineering*, 8 (1), (1971, 9).
- 5) T. Shinohara and K. Kubo, Experimental study on the lateral resistance of piles (I). *Reports of Transportation Tech. Research Inst.*, 11 (6), 1–74 (1961).
- 6) S. Tochiki and Y. Munekage, Study on fixing and mooring of cultivating fisheries equipment in the sea, *Reports of the studies for the shallow waters development*, 113–125 (1973, 4).

(Received : September 30, 1975)